Plasma Physics and
Controlled Fusion

PAPER • OPEN ACCESS

Exploring the use of low-temperature atmospheric plasma polymerization for the reduction of parasitic currents in type-II superlattice devices

To cite this article: R Gillies *et al* 2025 *Plasma Phys. Control. Fusion* **67** 025012

View the article online for updates and enhancements.

You may also like

- Performance modeling of MWIR InAs/GaSb/B–$Al_{0.2}Ga_{0.8}Sb$ type-II superlattice nBn detector
P Martyniuk, J Wróbel, E Plis et al.

- Antimonide-based high operating temperature infrared photodetectors and focal plane arrays: a review and outlook
Chunyang Jia, Gongrong Deng, Lining Liu et al.

- High speed antimony-based superlattice photodetectors transferred on sapphire
Arash Dehzangi, Ryan McClintock, Donghai Wu et al.

This content was downloaded from IP address 80.5.9.61 on 19/02/2025 at 16:23

OPEN ACCESS
IOP Publishing
Plasma Physics and Controlled Fusion
Plasma Phys. Control. Fusion **67** (2025) 025012 (6pp)
https://doi.org/10.1088/1361-6587/ada1fa

Exploring the use of low-temperature atmospheric plasma polymerization for the reduction of parasitic currents in type-II superlattice devices

R Gillies[1], K McKay[1,*], K Asku[1,3], V Srivastava[2], M Kersia[2] and I Sandall[1]

[1] Department of Electrical Engineering and Electronics, University of Liverpool, Liverpool L69 3GJ, United Kingdom
[2] School of Physics and Astronomy, Cardiff University, Cardiff CF24 3AA, United Kingdom
[3] National Tsing Hua University, Hsinchu, Taiwan

E-mail: k.mckay@liverpool.ac.uk

Received 5 August 2024, revised 3 December 2024
Accepted for publication 20 December 2024
Published 10 January 2025

Abstract
Type-II superlattice (T2SL) devices have the potential to be the new generation of semiconductor-based devices, however fabrication of these devices leads to surface defects that can create surface leakage channels. Passivation methods that are typically used in traditional semiconductors have proved unsuccessful. In this paper we present the initial findings of a low-temperature atmospheric pressure plasma polymerisation process capable of removing the unwanted oxide layers and depositing a thin layer of polymer to protect the surface. We examine the effect of monomer flow rate on the plasma optical emission and electrical characteristics and investigate the deposition chemistry. Finally, we demonstrate the effectiveness of the plasma treatment on T2SL devices and underpin the potential for this technique. These results were presented at the 50th IOP Plasma Physics Conference, April 2024.

Keywords: LTAP, T2SL, polymerisation, passivation, OES, FTIR-ATR, semiconductor

1. Introduction

Type-II superlattice (T2SL) is a periodic stack of two or more semiconducting layers theorised by Sai-Halasz *et al* [1]. It is considered one of the most promising III–V compound semiconductor-based alternatives to mercury cadmium Telluride. The bandgap tunability from 3–30 μm, achieved by tuning the thicknesses of the constituent layers in T2SL, has opened a world of possibilities [2–6]. This versatility has enabled the development of various devices, including photodetectors, light-emitting diodes, lasers, and phototransistors, sparking excitement in the field of infrared technologies. Emitters and detectors of T2SL find applications in spectroscopy, gas sensing, medical diagnostics, space and astronomy, defence, and night vision.

Over recent years, InAs/GaSb or InAs/InAsSb T2SL have been demonstrated as promising candidates for infrared detection [6–11]. In the standard approach to fabricating a diode pixel, mesa definition processes lead to abruptly terminated mesa side walls, which can cause the formation of unwanted oxide layers and band bending near the mesa walls, resulting in carrier accumulation. Freshly etched mesa sidewalls typically contain dangling bonds, inversion layers and interfacial traps [12, 13]. These surface defects in the

* Author to whom any correspondence should be addressed.

Original content from this work may be used under the terms of the Creative Commons Attribution 4.0 licence. Any further distribution of this work must maintain attribution to the author(s) and the title of the work, journal citation and DOI.

© 2025 The Author(s). Published by IOP Publishing Ltd

otherwise perfect crystal can create surface leakage channels. Various passivation methods, such as the deposition of dielectric layers (Silicon Nitride and Silicon Dioxide), are typically used in wide bandgap semiconductors to overcome surface leakage currents. However, such techniques have proved unsuccessful when applied to T2SLs, most likely due to multiple semiconductor materials, their relatively small bandgap and the relatively high deposition temperatures required to achieve a high-quality dielectric layer. This has led to polymer-based dielectrics being utilised in the best-performing T2SL devices reported. However, these devices still exhibit appreciable surface currents, even in large devices operating at room temperature [5].

Utilising a low-temperature atmospheric pressure plasma (LTAPP), we can not only clean/etch the semiconductor surface to remove any unwanted oxide layers, dangling bonds, etc, but also directly polymerise and deposit a range of possible passivation layers while maintaining low operating temperatures. Previous work has used LTAPPs to deposit peptides onto polymer surfaces for antibacterial applications and gas and surface phase polymerisation of monomers onto metals, plastics and dielectric materials [14]. 'Jet-type' plasma source configurations are particularly well suited for the treatment of semiconductors due to their small scale (∼few mm). They can treat complex surfaces and be rastered across a surface to cover larger-scale objects. Low-temperature atmospheric plasma polymerisation to reduce parasitic currents in T2SL devices is significant as it addresses a key challenge in infrared technologies and contributes to the global effort to combat environmental pollution caused by toxic gases such as carbon dioxide (CO_2), carbon monoxide (CO), methane (CH_4), nitrogen dioxide (NO_2), and nitric oxide (NO).

Here, we use a low-temperature atmospheric pressure plasma probe to polymerise acrylic acid monomer onto meso-etched InAs devices to examine the effect of this process on reducing surface currents. Monomer acrylic acid has a high vapour pressure making it easy to transfer into the gas phase and is widely used in its polymeric form. It has been shown previously to be easily polymerised by atmospheric pressure plasmas and has been widely studied making it a good initial test organic polymer for this study [15–18]. We present the initial findings, including a brief examination of the physio-chemical properties of the gas-phase plasma, the surface chemistry of the deposited polymer, and the effect of the treatment on the mesa-etched devices on the surface currents.

2. Experimental setup

The experimental set-up consists of a kHz signal generator (TTi TG1000 10 MHz) connected to an audio amplifier and a high voltage transformer (applied voltages: 6–8 kV, frequency: 10 kHz). This is then connected to the powered electrode positioned on the outside of the quartz tube 10 mm from the end (ID:3.6 mm, OD: 6 mm). A grounded central hollow needle electrode (inside the quartz tube) is connected to the He + AAc flow vessel (0–120 sccm), and a main He-only gas flow (2 SLM) fills the rest of the tube. A high-voltage probe (10 kV Testec HVP-15HF) and a Pearson current probe (model 2877) are used to monitor the applied current and voltage in conjunction with an oscilloscope (Tektronics TBS 1052B). As shown in figure 1. To obtain plasma current and voltage, IV waveforms are obtained when there is and is not a plasma discharge present, one is then subtracted from the other to provide the current and voltage dissipated in the plasma directly. These values are much smaller than the applied waveforms [19].

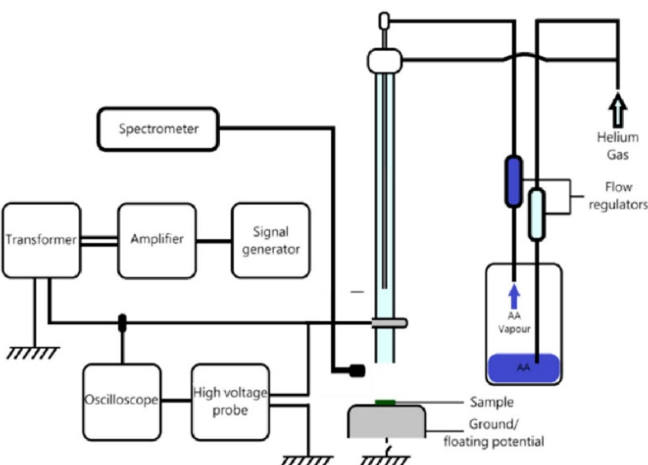

Figure 1. Plasma treatment setup.

To measure the gas-phase plasma chemistry *in situ*, an optical emission spectrometer (CMOS AvaSpec-ULS4096CL-EVO) with a 400 μm fibre was used to measure the plasma effluent. For the surface chemistry, a Jasco Fourier transform infrared spectrometer (FTIR) with a Pike attenuated total reflectance (ATR) accessory was used. Samples were placed on a grounded surface 15 mm below the tube exit, and for these initial studies the sample was stationary throughout the treatment time, i.e. single spot treatment. This is not ideal as the film thickness will vary as a function of distance from the treatment site, however it allows us to assess the effectiveness of treatment. In future work, the surfaces will be rastered to ensure a more homogeneous treatment.

Initial measurements were performed on blank InAs wafers. To create a roughened surface more representative of mesa device sidewalls, the wafer was etched for 30 s in a standard phosphoric acid, hydrogen peroxide and deionized water in a 1:1:1 ratio. To realise actual mesa diodes for characterising surface leakage currents, devices were patterned using standard contact photolithography, and Ti/Au (10/100 nm) contacts were deposited using thermal evaporation. T2SL devices were grown by molecular beam epitaxy using a Veeco Gern 930 reactor. The growth conditions for the T2SL p–i–n diodes are detailed in the [9, 10]. Current–voltage (I–V) measurements were performed by an Agilent Technology B1500A Semiconductor Device Analyser with a

current compliance limit of 5 mA, with the devices being directly probed via a probe station.

3. Results and discussion

3.1. Plasma characterisation using optical emission spectroscopy (OES) and plasma current and voltage measurements

Previous studies have examined the gas-phase chemistry produced during atmospheric pressure low-temperature polymerisation of acrylic acid and other monomers using mass spectrometry [20], while this is a very important technique for monitoring the polymerisation process, it is not suitable for *in-situ* measurements. Here we use OES and current and voltage measurement to monitor the general plasma conditions for different monomer flow rates and applied voltages when treating surfaces, in this case blank InAs wafers and mesa devices. Figure 2 provides an overview of the OES spectra collected at the exit of the quartz tube at an applied voltage of 7 kV for acrylic acid flow rates ranging from 0 sccm—120 sccm. As the flow rate increased, the plasma's overall light emission decreased. In figure 3, we plot individual lines that are representative of the Helium (706 nm), Nitrogen (391 nm, 337 nm) and Oxygen (777 nm) chemistry against flow rate for applied voltage from 6–8 kV. A general trend of decreasing intensity as a function of acrylic acid flow is again observed. This should be expected as more of the power goes to the polymerisation process rather than ionisation of the molecular and atomic states, and/or more of the reactive/excited species produced in the plasma are involved in the breaking of the double bonds in the monomer to produce then polymer chains [20]. However, for the 7 kV case we can see an increase in emission from 40 to 60 sccm. To understand what might be causing this increase in emission we examine the plasma current and voltage. In figure 4 we can see the plasma current and voltage, for fixed applied voltages of 6, 7 and 8 kV, versus the acrylic acid flow rate. In the 6 kV case, the plasma current and voltage have a minimum at 20 sccm, this is correlated with a very slight increase in optical emission (particularly the Helium and Oxygen lines), a further increase in emission is also observed at 40 sccm, where the current and voltage both increased. In the 7 kV case the minimum in current and voltage occurs at 60 sccm. This produces the very notable increase in the emission. For the 8 kV case, the current and voltage are minimum at 0 sccm, and both increase sharply at 20 sccm, in the optical emission a small increase is observed at 20 sccm but this is not as pronounced as in the other cases. In LTAP plasmas the plasma current can be related to electron density (free charge carriers) in the discharge [21], as the power dissipated in the plasma decreases, the electron density will decrease, meaning overall ionisation decreases, however, for Helium we know that intermediate states (metastables) play an important role in sustainment of the plasma discharge (lower energy requirements), if these states are involved in the radical chain breaking of the double bonds they are likely to emit a photon and de-excite. Hence, this could lead to an increase in light emission as these radicals and excited states interact with the monomers in the gas flow and lead to a decrease in electron density as there will be less ionisation occurring. While this requires more investigation, it is not within the scope of this work. When we treated the devices/wafers, we found that 7 kV and 60 sccm were the best conditions for deposition, so we are confident that this is an indication of enhanced polymerisation reactions.

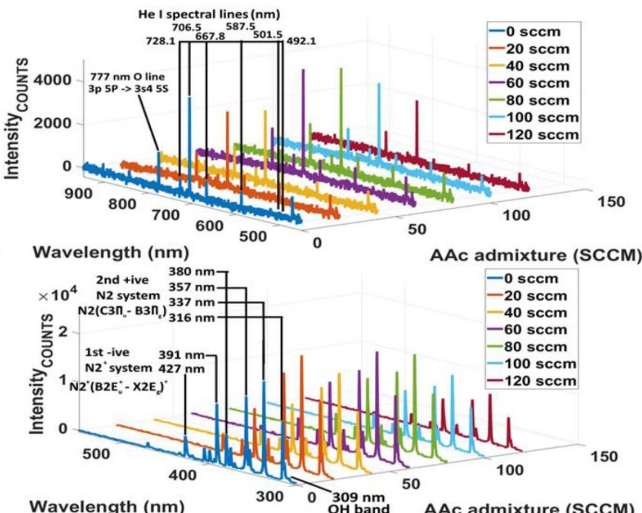

Figure 2. OES for He plasma with acrylic acid admixtures (0–120 sccm), at 7 kV and 10 kHz.

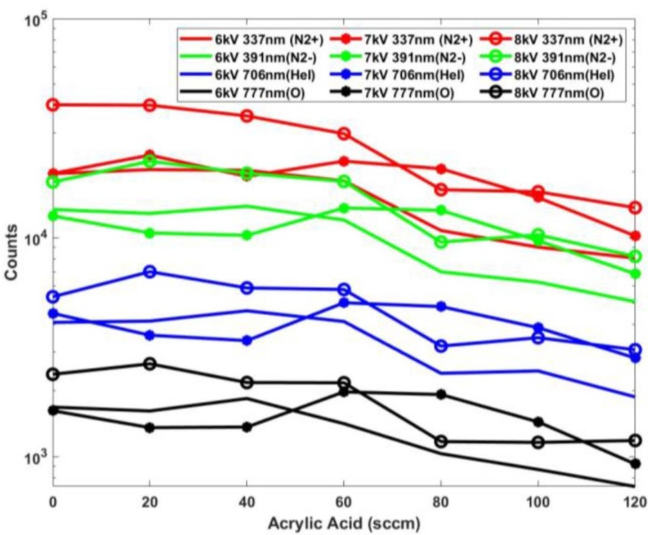

Figure 3. Individual OES lines (337 nm, 391 nm, 706 nm and 777 nm) for He plasma with acrylic acid admixtures (0–120 sccm), for 6–8 kV at 10 kHz.

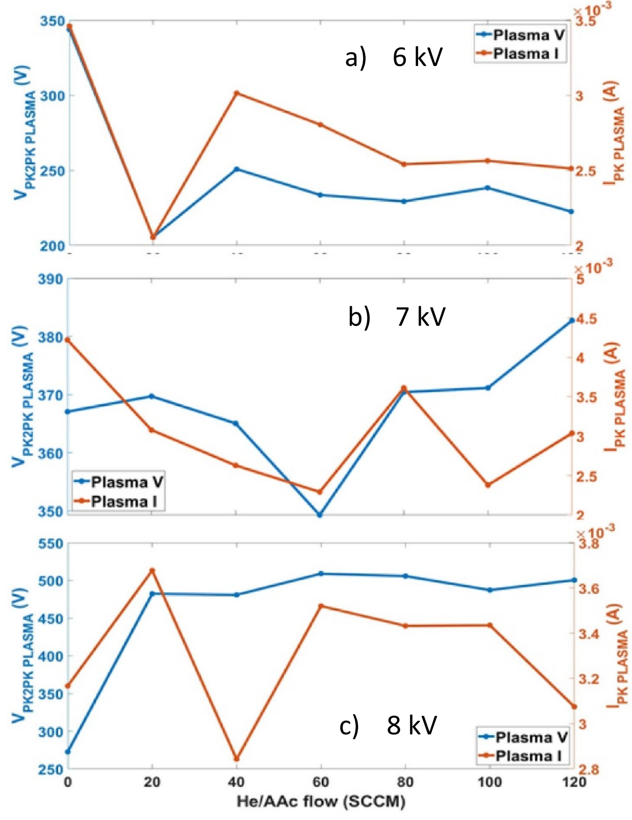

Figure 4. Plasma current (peak) and voltage measurement (pk–pk) for a 10 kHz He plasma with acrylic acid admixtures (0–120 sccm), for(a) 6 kV (b) 7 kV and (c) 8 kV.

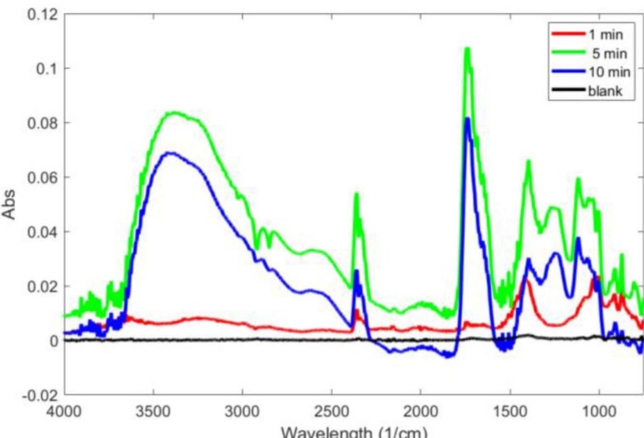

Figure 5. FTIR-ATR for 7 kV He + AAc plasma (60 sccm) on InAs wafers for treatment times of 1, 5 and 10 mins (+1 min plasma only pre-treatment). Blank included for comparison. None of this data has been baseline corrected.

3.2. FTIR-ATR plasma polymerised surfaces

To examine the effect of plasma treatment time on the polymer layer formed on blank InAs wafers, we used FTIR-ATR. Figure 5 shows the results for treatment times of 1, 5, and 10 min, a blank sample is also included, for 7 kV and 60 sccm (please note these have not been baseline corrected—and are just to determine if we have the AAc polymer signature). Please note that as we have single spot treatment, the film thickness varies over the surface as a result the 5 and 10 min treatments show different intensities, suggesting a thicker film on the 5 min samples but this is just an artifact of where the FTIR-ATR made contact with the samples, here we are interested in the signal shape (i.e. do we see the polymer peaks). The acrylic acid polymer signal can be seen clearly after 5 min of treatment (green). After 1 min a change in the surface chemistry can be seen when compared to the blank, but it is does not have all the characteristic peaks (i.e. C=O $\sim$1717 cm^{-1}, OH stretching $\sim$3500–2500 cm^{-1}, etc) of the polymer [22]. Instead, peaks can be seen at 2359 cm^{-1} (CO_2), 1418 cm^{-1} (potentially COO^- symmetric peak) and 1007 cm^{-1}, the $\sim$3750–2500 cm^{-1} region might indicate the OH stretching region, C–H and O–H/C–O peaks but this is not conclusive in these measurements. While the main peaks cannot be directly linked to the polymer they are evidence of changes to the surface chemistry, there appearance in the 5 min and 10 min spectra also reassures us that this is due to the surface treatment. Visually, after short treatment times, there is also a change in the light reflected from the surface where the polymer is. This suggests that the coatings are on the nm scale, as the FTIR performs best when coatings are on the order of μm. For the mesa devices treatment times were kept below 5 min and the surfaces were grounded to prevent excessive charge build up. Due to the non-flat surface, however, these could not be measured without damaging the surface using the FTIR-ATR.

3.3. IV measurements of treated devices

To determine the effect of plasma treatment on the devices, we treated several samples under various conditions. Here we examine the effect of plasma only and plasma/polymer treatments. Figure 6 shows the dark current density (current divided by device area) versus applied voltage for different-sized devices after etching but with no plasma treatment. If devices do not suffer from surface leakage, their current densities under reverse bias will scale with the device area. As can be observed here, there is significant disagreement in the measured currents for the different-sized devices, clearly evidencing the presence of surface leakage currents. Figure 7 shows the current density as a function of applied bias for devices passivated with Acrylic Acid with an applied voltage of 7 kV and a flow rate of 60 sccm. The figure shows the results for devices positioned within 0.5 mm of the jet nozzle. Excellent agreement between devices of differing sizes can be observed, indicating that bulk leakage currents dominate devices and that the parasitic surface leakage currents have been successfully suppressed. The demonstration of purely bulk current at room temperature demonstrates that AAc can be at least as effective at passivation as those currently used in the literature [5], however further testing and evaluation beyond the scope of this initial proof of concept is required to determine if it is superior in terms of temperature performance, scalability and lifetime. To investigate the influence of the plasma deposition jet's

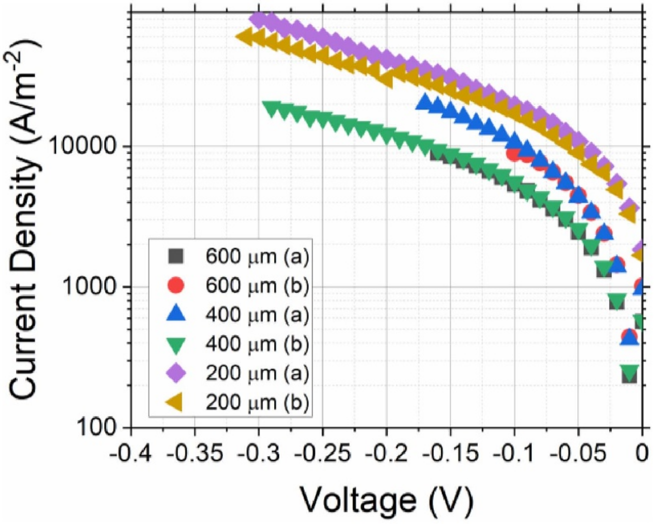

Figure 6. Dark current density (*I*/*A*) vs applied voltage of T2SL devices prior to plasma treatment.

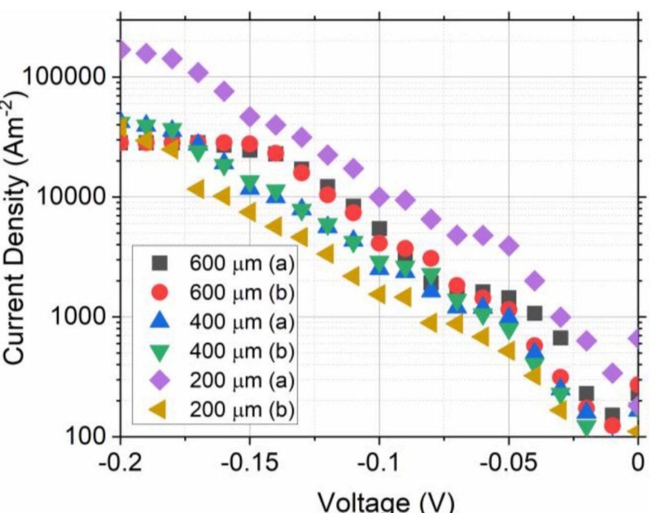

Figure 8. Dark current density (*I*/*A*) vs applied voltage of T2SL devices between 0.5 mm −1 mm from 7 kV plasma treatment (1 min plasma only + 1 min plasma + AAc (60 sccm)).

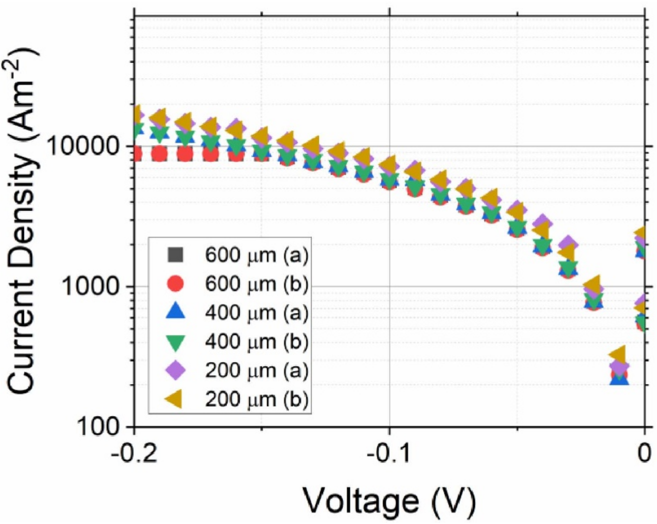

Figure 7. Dark current density (*I*/*A*) vs applied voltage of T2SL devices within 0.5 mm of 7 kV plasma treatment (1 min plasma only + 1 min plasma + AAc (60 sccm)).

position on the passivation's effectiveness, figure 8 shows the current density for different-sized devices that were positioned between 0.5 and 1 mm away from the centre of the plasma jet. There is now a significant disagreement between devices of different sizes, indicating that the devices have a substantial amount of surface leakage current.

These results indicate that the device's position being passivated relative to the plasma jet is a critical parameter that needs to be controlled and evaluated to enable successful passivation. This is most likely due to the Acrylic Acid forming a mountain-type topology under the plasma jet, with the devices directly under the jet encountering a much thicker layer than more peripheral devices. Similarly, the devices directly under the jet will also have had a longer exposure time to the He plasma, resulting in a different amount of surface etching before the Acrylic Acid deposition. These processes are likely further complicated due to the very non-planar topology of the semiconductor wafer, with the etched mesa's forming different-sized islands with heights of several microns and varying device-to-device spacing resulting in a difficult-to-model or predict gas flow around them as well as shadowing effects. Therefore, to be utilised as an effective, controllable and repeatable passivation process in the manufacture of semiconductor devices, either the sample will need to be moved via an appropriate stage during the process or a much wider jet will need to be utilised to ensure that the process is uniform across all devices.

During the plasma deposition, there are two separate processes occurring to the surface. Firstly, the He plasma will interact with the surface potentially providing an etch to the semiconductor surface or any native oxide present. This will then be followed by the Acrylic Acid deposition itself which may then passivate any dangling bonds as well as providing an encapsulation layer to preserve the condition of the surface and prevent reoxidation. From the results shown so far we can only evaluate the end effect of these two processes and not the individual contribution of each. To try and decouple these processes we have also undertaken a test where a sample was exposed to a 1 min He plasma, with no Acrylic Acid flow. The device IVs were then immediately measured (although with no vacuum transport of the samples between apparatus) to evaluate the performance after the He etch but before the Acrylic Acid deposition. The results shown in figure 9 indicate that while the responses from differently sized mesas are closer together than in the initial untreated case, there is still significant disagreement between them and overall the performance is sub-standard compared to the device which experienced plasma deposition and Acrylic Acid. This result indicates that the initial He plasma improves the surface condition,

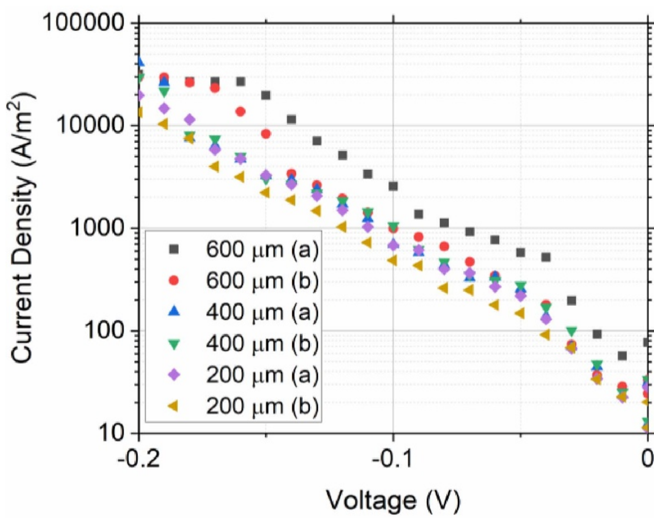

Figure 9. Dark current density (*I*/*A*) vs applied voltage of T2SL devices within 0.5 mm from 7 kV plasma treatment (1 min plasma only)).

most likely via the etching of native oxide layers, however the subsequent Acrylic Acid deposition is still required for either further passivation of dangling bonds or to protect the surface from reoxidation and further reactions.

4. Conclusions

In this paper we have presented initial results which highlight the potential of using a LTAPP polymerisation process for the passivation of T2SLs. Using OES and electrical measurements we have shown that there are measurable changes in emission profiles which relate to changes in the plasma current and voltage. This can cautiously be related to polymerisation conditions, with an applied voltage of 7 kV and monomer flow rate of 60 sccm providing the best coating conditions. Fourier transform infrared spectroscopy with ATR was used to measure the coating chemistry to assess the appropriate treatment time. Treatment time of 5 min (+1 plasma only) showed clear evidence of polyacrylic acid formation and the 1 min (+1 plasma only) treatment showed changes in the surface chemistry (primarily the CO_2 peak and a small increase in the OH stretching band) and visibly changes in the surface reflectance where seen, it was believed that coatings on the order of nm were achieved even with short treatment times. Keeping treatment <5 min reduces the surface charge accumulation and ensures that the devices are not damaged.

We have successfully shown that plasma polymerisation of the T2SL devices supresses parasitic surface leakage currents. The need for homogenous coatings across the surface is clear from the results which show poorer performance of devices >0.5 mm away from the active area of the plasma. The effect of the plasma only and the polymerised acrylic acid treatments were also discussed, and while plasma only has a measurable effect on the performance of the devices, this is enhanced by the polymerisation process.

Data availability statement

The data cannot be made publicly available upon publication. The data that support the findings of this study are available upon reasonable request from the authors.

Acknowledgment

We acknowledge financial support for the Defence and Security Accelerator under Contract ACC2024551.

ORCID iDs

R Gillies https://orcid.org/0009-0001-4787-9361
K McKay https://orcid.org/0000-0003-1822-7994
K Asku https://orcid.org/0009-0006-5763-5375

References

[1] Sai-Halasz G A, Tsu R and Esaki L 1977 *Appl. Phys. Lett.* **30** 651
[2] Rogalski A, Martyniuk P and Kopytko M 2017 *Appl. Phys. Rev.* **4** 031304
[3] Meng C, Li J, Yu L, Wang X, Han P, Yan F, Xu Z, Chen J and Ji X 2020 *Opt. Express* **28** 14753–61
[4] Alshahrani D O, Kesaria M, Anyebe E A, Srivastava V and Huffaker D L 2022 *Adv. Photon. Res.* **3** 2100094
[5] Kwan D, Kesaria M, Anyebe E A and Huffaker D 2021 *Infrared Phys. Technol.* **116** 103756
[6] Keen J A, Lane D, Kesaria M, Marshall A R J and Krier A 2018 *J. Phys. D: Appl. Phys.* **51** 075103–12
[7] Keen J A, Repiso E, Lu Q, Kesaria M, Marshall A R J and Krier A 2018 *Infrared Phys. Technol.* **93** 375–80
[8] Kwan D, Kesaria M, Anyebe E A, Alshahrani D O, Delmas M, Liang B L and Huffaker D L 2021 *Appl. Phys. Lett.* **118** 203102
[9] Kesaria M, Alshahrani D, Kwan D, Anyebe E and Srivastava V 2021 *Mater. Res. Bull.* **142** 111424
[10] Kwan D, Kesaria M, Jiménez J J, Srivastava V, Delmas M, Liang B L, Morales F M and Huffaker D L 2022 *Sci. Rep.* **12** 11616
[11] Alshahrani D, Kesaria M, Jiménez J J, Kwan D, Srivastava V, Delmas M, Morales F M, Liang B and Huffaker D 2023 *ACS Appl. Mater. Interfaces* **15** 8624–35
[12] Jaouad A, Aimez V and Aktik C 2004 *IET Electron. Lett.* **40** 1024
[13] Jaouad A and Aimez V 2006 *Appl. Phys. Lett.* **89** 092125
[14] Aveyard J, Bradley J W, McKay K, McBride F, Donaghy D, Raval R and D'Sa R A 2017 *J. Mater. Chem.* B **5** 2500–10
[15] Fahmy A, Mix R, Schönhals A and Friedrich J F 2011 *Plasma Process. Polym.* **8** 147–59
[16] Fahmy A, Mohamed T A and Schönhals A 2015 *Plasma Chem. Plasma Process.* **35** 303–20
[17] Topala I, Dumitrascu N and Popa G 2009 *Nucl. Instrum. Methods Phys. Res.* B **267** 442–5
[18] Bitar R, Cools P, De Geyter N and Morent R 2018 *Appl. Surf. Sci.* **448** 168–85
[19] Jovanović O, Puač N and Škoro N 2022 *Plasma Sci. Technol.* **24** 105404
[20] Moix F, McKay K, Walsh J L and Bradley J W 2015 *Plasma Process. Polym.* **13** 236–40
[21] Yambe K, Saito H and Ogura K 2015 *IEEJ Trans. Electr. Electron. Eng.* **10** 614–8
[22] Kirwan L, Fawell P D and van Bronswijk W 2003 *Langmuir* **19** 5802–7